

Beyond Topology: A Lagrangian Metaphor to Visualize the Structure of 3D Tensor Fields

Xavier Tricoche, Mario Hlawitschka, Samer Barakat, and Christoph Garth

Abstract Topology was introduced in the visualization literature some 15 years ago as a mathematical language to describe and capture the salient structures of symmetric second-order tensor fields. Yet, despite significant theoretical and algorithmic advances, this approach has failed to gain wide acceptance in visualization practice over the last decade. In fact, the very idea of a versatile visualization methodology for tensor fields that could transcend application domains has been virtually abandoned in favor of problem-specific feature definitions and visual representations. We propose to revisit the basic idea underlying topology from a different perspective. To do so, we introduce a Lagrangian metaphor that transposes to the structural analysis of eigenvector fields a perspective that is commonly used in the study of fluid flows. Indeed, one can view eigenvector fields as the local superimposition of two vector fields, from which a bidirectional flow field can be defined. This allows us to analyze the structure of a tensor field through the behavior of fictitious particles advected by this flow. Specifically, we show that the separatrices of 3D tensor field topology can in fact be captured in a fuzzy and numerically more robust setting as ridges of a trajectory coherence measure. As a result, we propose an alternative structure characterization strategy for the visual analysis of practical 3D tensor fields, which we demonstrate on several synthetic and computational datasets.

1 Introduction and Motivation

Tensor fields are ubiquitous in the theory of continuum mechanics. They offer an elegant mathematical language to describe the forces acting upon solids and fluids. Their analysis is therefore needed in application disciplines ranging from structural mechanics and fluid dynamics to geophysics, earthquake research, materials engineering, and aeronautics. The theoretical and practical importance of tensor fields has led to a dedicated research effort in the scientific visualization community aimed

Xavier Tricoche
Purdue University, e-mail: xmt@purdue.edu

Mario Hlawitschka
University of California at Davis, e-mail: hlawitschka@ucdavis.edu

Samer Barakat
Purdue University, e-mail: sbarakat@purdue.edu

Christoph Garth
University of California at Davis, e-mail: cgarth@ucdavis.edu

at devising analysis tools that allow scientists and engineers to make sense of the corresponding datasets. Yet, the task is challenging owing to the size, dimensionality, and many degrees of freedom of the data.

To address this difficulty, a general approach in the visualization literature consists in extracting salient structures from the data in a pre-processing stage. The information obtained through this computation is then used to facilitate the visual inspection of large and complex datasets. Specifically, it allows subsequent data depictions to focus on remarkable geometric descriptors, thus avoiding visual clutter while improving the interactivity of the visualization. Topology in particular provides a theoretical framework within which the notions of structure and saliency can be articulated in a principled way. Following the introduction of this formalism in vector field visualization, topology was extended to tensor fields over 15 years ago and a complete algorithmic framework is now available for the extraction of the so-called topological skeleton in three-dimensional datasets [18].

One could therefore assume that a general solution has been found to the visual analysis of 3D tensor fields. Unfortunately, a rapid glance at the recent literature reveals unambiguously that topology has fallen short of offering a globally valid approach for this problem and it has not been adopted by visualization practitioners in the investigation of their tensor data. The shortcomings of the topological approach in 3D concern its significant algorithmic complexity and its lack of numerical robustness. The latter aspect is particularly problematic since it essentially disqualifies this method from being applied to any measured or simulated numerical dataset. Instead, the characterization of important structures in application datasets has been mainly driven by domain-specific feature of interest that lack generality and are typically defined in an ad-hoc manner. A prime example of this trend concerns the large body of work dedicated to diffusion tensor imaging (DTI) data, where anatomical structures such as fiber bundles are the natural focus of both analysis and visual representation.

We propose in this paper to revisit the basic idea underlying topology from a different perspective. Specifically, we introduce a Lagrangian metaphor that transposes to the structural analysis of eigenvector fields a mathematical theory that has recently gained popularity in the fluid dynamics community. Building upon the strong theoretical connections that exist between vector and eigenvector fields, we show that the topology of 3D tensor fields can be characterized through extremal manifolds of a trajectory coherence measure obtained by processing eigenvector fields. This approach significantly improves upon the topological method however in that it yields a fuzzy and numerically more robust characterization that is well suited for practical datasets. We demonstrate our technique and compare the extracted structures to topology in a benchmark analytical datasets and in a computational fluid dynamics simulation. Our results document the potential of this general strategy for the visual analysis of symmetric 3D tensor fields across engineering and scientific applications.

The remainder of this paper is organized as follows. We review previous work in tensor field visualization with an emphasis on the topological framework in Section 2. The theoretical foundations of our approach, which span dynamical systems,

differential geometry, and computer vision, are summarized in Section 3. The proposed model of structure is described in Section 4 along with some algorithmic considerations. Finally, results are shown in Section 5 and we point out promising avenues for future research in Section 6.

2 Related Work

2.1 Topological methods

The topological framework was first applied to the visualization of second-order tensor field by Delmarcelle and Hesselink [4]. Leveraging ideas introduced previously for the topology-based visualization of vector fields [12, 9], these authors proposed to display a planar tensor field through the topological structure of its two orthogonal eigenvector fields. As discussed in their work, the lack of orientation of eigenvector fields leads to singularities that are not seen in regular vector fields. Indeed, those *degenerate points* correspond to locations where the tensor field becomes isotropic, i.e. where both eigenvalues are equal and the eigenvectors are undefined. Yet, this seminal work shows that a similar synthetic representation is obtained in the tensor setting through topological analysis: degenerate points are connected in graph structure through curves called *separatrices* that are everywhere tangent to an eigenvector field. Refer to Figure 1.

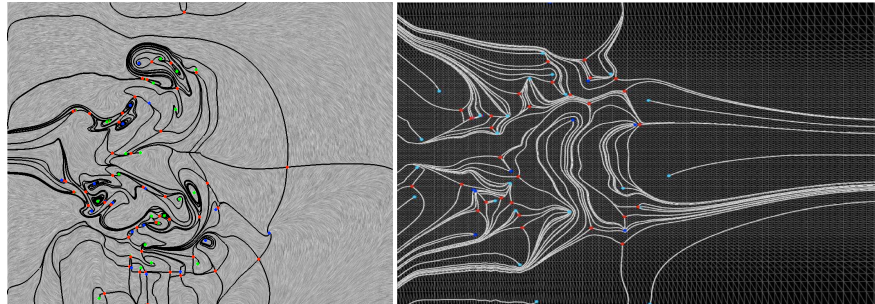


Fig. 1 Topological graph. Singularities correspond to the nodes of the graph, while separatrices form the edges. Left: vector field topology of a turbulent flow. Right: topology of a rate of strain symmetric tensor field.

The three-dimensional case was first considered in a subsequent paper by Hesselink *et al.* [13]. Interestingly, their discussion was primarily focused on the types of degenerate *points* that can occur in this setting. As such it did not explicitly mention that the most typical singularities in 3D are lines and not isolated points. In fact, this basic property was first pointed out in the work of Zheng and Pang [34] who also proposed the first algorithm for the extraction of these line features. In a nutshell,

their method consists in computing the intersection of these lines with the faces of a voxel grid, by solving a set of 7 cubic equations. This method was later improved by allowing for the continuous tracking of intersection points across the voxel interior [35]. Additionally, a geometric formulation was proposed as an alternative to the system of equations [35]. Most recently, Schultz *et al.* discussed three-dimensional tensor field topology in the context of DT-MRI data [27]. Following a systematic approach, their work demonstrates the shortcomings of this mathematical framework in the structural analysis of the typically noisy images acquired in practice. As an alternative, they proposed an approach where structure is defined with respect to a stochastic assessment of the connectivity along integral curves.

2.2 Ridges and valleys

The detection of creases, in other words ridges and valleys, in scalar images is a topic of traditional interest in a variety of disciplines, most prominently in image processing and computer vision [17]. Among the multiple definitions proposed in the literature, the one introduced by Eberly *et al.* is widely used in practice [5]. In essence, this definition generalizes the intuitive height-based definition of ridges and valleys [3] to d -dimensional manifolds embedded in n -dimensional image space [6].

From an algorithmic standpoint, several methods have been proposed that permit the extraction of these manifolds from numerical data. Many of them apply a principle similar to Marching Cubes [19], effectively interpreting creases as 0-level sets of the dot product between the gradient of the considered scalar image and one or several eigenvectors of its hessian matrix. The lack of intrinsic orientation of those eigenvectors requires the use of heuristics to provide them with an arbitrary but locally consistent orientation. Some authors match sets of eigenvectors across the faces of a voxel [21] while others determine a local reference by computing the average orientation of the eigenvector field over a face [30]. A scale-space approach is discussed in [8]. Peikert and Roth introduced the notion of *Parallel Vector Operator* [22] as a computation primitive in flow visualization and they showed that it could be used to find the intersection of ridge and valley lines with the faces of a computational mesh [23]. Computationally, the method can be implemented in a variety of ways, including isocontour intersection, iterative numerical search, and through the solution of an eigensystem.

It is interesting to observe that several applications of this general methodology to Scientific Visualization problems have been presented in recent years. Sahner *et al.* extract a skeleton of vortices in three-dimensional flows as valley lines of a Galilean invariant (invariant under changes of inertial reference frame) called λ_2 [25]. Their algorithm combines ideas developed by Eberly with a *Feature Flow Field* approach [31]. In a work most closely related to ours, Kindlmann *et al.* extract ridge and valley surfaces of the *Fractional Anisotropy* (FA) in DTI volumes using a modified version of *Marching Cubes*. In particular, their scheme uses smooth reconstruction kernels and an orientation tracking scheme along edges to assign a

coherent orientation to an eigenvector field on a voxel face. In addition, Sadlo and Peikert applied the scheme proposed by Furst and Pizer [7] to extract *Lagrangian Coherent Structures* from transient flows as ridge and valley surfaces of a scalar measure of particle coherence [24].

3 Theory

We review in this section the two major models proposed to date in the visualization literature to identify salient structures in tensor fields, namely topology and creases, and underscore their connections. In doing so, we explicitly restrict our considerations to techniques applicable to a broad range of applications and as such do not assume a specific physical interpretation for the tensor field. We then briefly introduce the notion of Lagrangian coherent structures, which has recently attracted significant attention in the fluid dynamics community and stems from the theory of dynamical systems. Finally, we describe how this conceptual framework can be extended to apply to tensor field, a generalization that we justify by the mathematical link that exists between vector and line fields.

Tensor Field Topology

A three-dimensional second-order symmetric tensor (simply called *tensor* hereafter) is fully represented by its three real eigenvalues (*tensor shape*) and an associated set of mutually orthogonal eigenvectors (*tensor orientation*). For a tensor field, the ordering of the three eigenvalues $\lambda_1 \geq \lambda_2 \geq \lambda_3$ thus defines *major*, *medium*, and *minor* eigenvector fields. Because such fields carry neither norm nor intrinsic orientation, they form *line fields*. In each eigenvector field, one can define curves that are everywhere tangent to the field. These curves are generally referred to as *hyperstreamlines* in the visualization literature [4].

One can characterize the topology of an eigenvector field in terms of the connectivity established by its hyperstreamlines. In other words, topology segments the domain into regions where hyperstreamlines share the same end points. This formalism is directly related to the topological framework used to study vector fields, where it characterizes regions of similar asymptotic behavior of the corresponding flow [26]. Note that the three eigenvector fields associated with a tensor field are mutually orthogonal and their topologies are closely related.

In the tensor setting, singularities of the topology corresponds to locations where the directional information of an eigenvector field is degenerate, which occurs when two or more eigenvalues are equal. Three degenerate configurations are possible in 3D, namely $\lambda_1 = \lambda_2 > \lambda_3$ (*planar anisotropy*), $\lambda_1 > \lambda_2 = \lambda_3$ (*cylindrical anisotropy*), and $\lambda_1 = \lambda_2 = \lambda_3$ (*spherical isotropy*). While the latter case is in fact numerically unstable and typically absent from practical datasets, the first two de-

generacies are stable features of the tensor topology. In their recent work Zheng and Pang have shown that these features are in general lines [34, 35].

A major drawback of the topological approach lies in its lack of robustness. Indeed, the structures identified by a topological analysis are very sensitive to noise and therefore essentially meaningless in the context of measured data such as Diffusion Tensor Imaging (DTI), where low signal-to-noise are typical in clinical practice [27]. This result echoes our observation that alternative structure definitions are needed to address the visual analysis needs of a variety of problems. We illustrate this point with our results on FA in DTI in section 5.

Crease Manifolds in Tensor Fields

The ridges and valleys (collectively, creases) of a scalar field f can be defined in terms of the gradient $\mathbf{g} = \nabla f$ and Hessian \mathbf{H} of the field [6]. In other words, creases are the manifolds along which f is at a local extremum, when constrained to the line or plane defined by one or two eigenvectors of the Hessian. A function is at extrema where its gradient is orthogonal to the constraint surface [20], thus ridges and valleys are where the gradient \mathbf{g} is orthogonal to one or two of the unit-length eigenvectors $\{\mathbf{e}_1, \mathbf{e}_2, \mathbf{e}_3\}$ (with corresponding eigenvalues $\lambda_1 \geq \lambda_2 \geq \lambda_3$) of the Hessian \mathbf{H} :

	Surface	Line
Ridge	$\mathbf{g} \cdot \mathbf{e}_3 = 0$ $\lambda_3 < 0$	$\mathbf{g} \cdot \mathbf{e}_2 = \mathbf{g} \cdot \mathbf{e}_3 = 0$ $\lambda_3, \lambda_2 < 0$
Valley	$\mathbf{g} \cdot \mathbf{e}_1 = 0$ $\lambda_1 > 0$	$\mathbf{g} \cdot \mathbf{e}_1 = \mathbf{g} \cdot \mathbf{e}_2 = 0$ $\lambda_1, \lambda_2 > 0$

Observe that the sign and the magnitude of the eigenvalue(s) determine the crease strength. In particular, $|\lambda_1|$ (resp. $|\lambda_2|$) measure the feature strength of a valley line (resp. surface), while $|\lambda_3|$ (resp. $|\lambda_2|$) measure the feature strength of a ridge line (resp. surface) [6].

A link between creases and tensor fields can be established through the study of scalar invariants. Invariants of second-order three-dimensional tensors can be intuitively understood as measurements of tensor *shape*, which is independent of tensor *orientation*. As such, they are defined in terms of the tensor's eigenvalues. In particular, an invariant called *mode* [2] provides a conceptual link between creases and tensor field topology [32] while the ridge manifolds of FA have been shown to delineate the one- and two-dimensional core structures of major fiber bundles in the brain white matter, and valley surfaces of FA constitute boundaries between adjacent fiber bundles with distinct orientations [16, 32, 28, 15].

We show in the following that creases can be applied to the direction information of a tensor field to reveal salient manifolds that relate to the topological skeleton.

Lagrangian Coherent Structures

As a preamble to the Lagrangian definition of structure for tensor fields that we discuss in the next section, we briefly introduce in the following the notion of Lagrangian coherent structures in vector fields. The conceptual link between these two structure types is established in Section 4.1 through the interpretation of an eigenvector field as a bidirectional flow.

A vector field \mathbf{v} can be associated with a *dynamical system* through following equations.

$$\begin{cases} \dot{\mathbf{x}}(t, t_0, \mathbf{x}_0) = \mathbf{v}(t, \mathbf{x}(t, t_0, \mathbf{x}_0)) \\ \mathbf{x}(t_0, t_0, \mathbf{x}_0) = \mathbf{x}_0, \end{cases}$$

where the dot designates derivation with respect to the time variable t , \mathbf{x}_0 is the *initial condition*. The trajectory $\mathbf{x}(\cdot, t_0, \mathbf{x}_0) : t \mapsto \mathbf{x}(t, t_0, \mathbf{x}_0)$ is obtained by integrating the system. The map $\mathbf{x}_t := \mathbf{x}(t, t_0, \cdot)$ is called *flow map*: $\mathbf{x}_t(\mathbf{x}_0)$ corresponds to the position reached at time t by a particle released at \mathbf{x}_0 at time t_0 .

The coherence of particle trajectories can be quantified through the *finite-time Lyapunov exponent* (FTLE) [11]. Specifically, stable and unstable *Lagrangian coherent structures* (LCS) are characterized as ridge manifolds of the FTLE field. With previous notation, one considers the flow map \mathbf{x}_T which maps a position \mathbf{x}_0 occupied by a particle at initial time t_0 to the position reached by this particle at time $T = t_0 + \tau$, where τ is finite. The spatial variations of this flow map around a given position \mathbf{x}_0 are locally determined by its spatial gradient, the Jacobian matrix $J_{\mathbf{x}}(t, t_0, \mathbf{x}_0) := \nabla_{\mathbf{x}_0} \mathbf{x}(t, t_0, \mathbf{x}_0)$ at \mathbf{x}_0 . This gradient can be used to determine the maximal dispersion after time τ of particles in a neighborhood of \mathbf{x}_0 at time t_0 as a function of the direction \mathbf{d}_{t_0} along which we move away from \mathbf{x}_0 : $\mathbf{d}_t = J_{\mathbf{x}}(t, t_0, \mathbf{x}_0) \mathbf{d}_{t_0}$. Maximizing the norm $|\mathbf{d}_t|$ over all possible unit directions \mathbf{d}_{t_0} corresponds to computing the spectral norm of $J_{\mathbf{x}}(t, t_0, \mathbf{x}_0)$ (i.e., the square root of the maximum eigenvalue of $J^T J$). Therefore, maximizing the dispersion of particles around \mathbf{x}_0 at t_0 over the space of possible directions around \mathbf{x}_0 is equivalent to evaluating

$$\sigma_\tau(t_0, \mathbf{x}_0) := \sqrt{\lambda_{\max}(J_{\mathbf{x}}(t, t_0, \mathbf{x}_0)^T J_{\mathbf{x}}(t, t_0, \mathbf{x}_0))}. \quad (1)$$

Linearization and normalization by advection time τ yields following expression for the finite-time Lyapunov exponent:

$$\lambda(t, t_0, \mathbf{x}_0) = \frac{1}{|\tau|} \log \sqrt{\lambda_{\max}(J_{\mathbf{x}}(t, t_0, \mathbf{x}_0)^T J_{\mathbf{x}}(t, t_0, \mathbf{x}_0))}. \quad (2)$$

This rate can be evaluated for both forward and backward advection (positive or negative τ). Large values of λ for forward (resp. backward) advection correspond to unstable (resp. stable) manifolds with repelling (resp. attracting) impact on nearby particles.

It is key to note that the separatrices of the topology belong to the hyperbolic manifolds that are characterized as LCS. Therefore the structures that are identi-

fied in numerical datasets using the standard topological method can typically be characterized in the LCS framework. The LCS method is also more robust to noise and uncertainty since it defines structures as the ridge surfaces of a continuously varying measure. Hence, the LCS approach provides a conceptual framework that elegantly generalizes the topological method while overcoming some of its most basic limitations in visual data analysis.

4 A Lagrangian Model of Structure in Tensor Fields

4.1 An Extension of LCS to Tensor Fields

As previously defined, LCS and FTLE are notions that pertain only to vector fields. Yet, visualization research has successfully exploited the connections between vector and eigenvector fields. A profound mathematical link exists between vector fields and so-called *line fields* (in other words a field associated each point with a line direction [29]), of which eigenvector fields are a particular example. This connection can be intuitively understood by considering the projection that associates a vector field defined over a *2-fold covering space* and a line field. *Branching points* in the covering result in (topological) singularities. Refer to Figure 2.

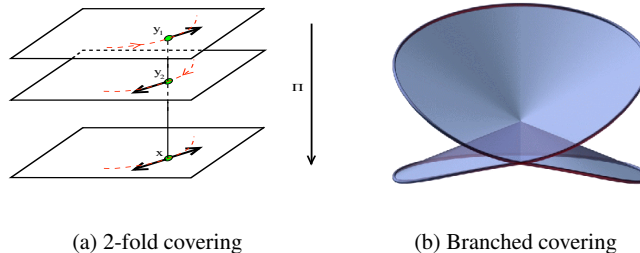


Fig. 2 Covering spaces provide a theoretical connection in the form of a *projection* between a vector field defined over a self intersecting 2-manifold embedded in a 3D *ambient space* and a 2D eigenvector field.

It was shown in previous work [26, 33] that it provides a high-level theoretical justification for the transposition of the topological (and other vector field visualization approaches) to the study of eigenvector fields. In the light of the parallel drawn in Section 3 between LCS and vector field topology, this fundamental connection permits an extension of the notion of LCS to tensor fields.

To provide a more formal motivation for this generalization, it is necessary to consider the definition of the separatrices in the topological skeleton of a tensor

field. In the 3D case, these separatrices are two-dimensional manifolds that originate along the 1D singularities. More specifically, these manifolds form in the vicinity of the singularity the boundary of so-called hyperbolic sectors [33, 37]. Refer to Figure 3 for an illustration of the possible sector types. It is the dispersion of the

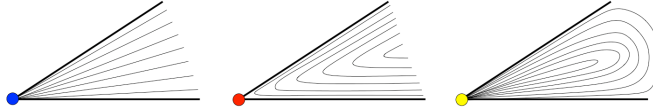


Fig. 3 Sector types in the vicinity of a singularity correspond to different patterns formed by integral curves. Left: parabolic type. Center: hyperbolic type. Right: elliptic type. These patterns are the only possible ones.

hyperstreamlines in the vicinity of separating manifolds that enables their characterization as ridges of a measure similar to FTLE.

Eigenvector fields do not possess an orientation and the presence of singularities in the topology clearly makes a globally consistent orientation of hyperstreamlines impossible in general. However, such an orientation can be assigned locally to yield a partial vector field and associated flow. The magnitude of this vector field is meaningless and can be considered normalized. Observe that the construction we just described is in fact the one that is implicitly taking place when hyperstreamlines are being constructed through numerical integration: a vector field is locally fitted to the underlying line field to advance the integration. With that setup in place, we can now define a finite-time Lyapunov exponent computed in this locally valid vector field. Refer to Figure 4 for an illustration of this procedure.

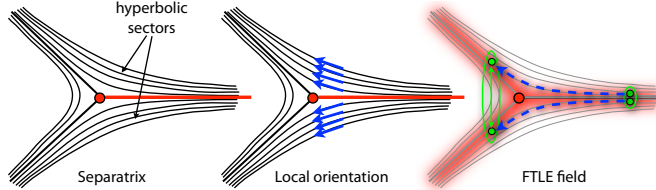


Fig. 4 FTLE computed in a locally defined and normalized vector field that is everywhere tangent with the underlying eigenvector field.

Like the standard FTLE definition, this construction yields two values σ_1 and σ_2 at any domain location, corresponding to a measure of dispersion rate of the local flow in either direction. In contrast to a real flow however, the lack of globally consistent orientation of this piecewise defined vector fields makes it impossible to globally distinguish between these two directions. A simple solution to this problem however consists in selecting the maximum of both measures $\sigma_{max} = \max(\sigma_1, \sigma_2)$, thus effectively revealing the underlying salient hyperbolic manifolds.

The second fundamental difference between a vector and an eigenvector field from the point of view of this structure characterization concerns the eigenvectors' lack of intrinsic norm. The local vector field mentioned previously can be assumed to be normalized. This, in turn, means that the integration time τ present in the definition of FTLE (Equation 1) amounts to a spatial length in this context. This new meaning suggests that this parameter should in fact be considered as a scale parameter. We discuss the practical implications of this observation in further detail in the following sections.

4.2 Computation

The computation of LCS requires the integration of tangent curves in the considered field from a dense set of locations distributed over the domain of definition. In the context of tensor fields, the integration must be carried out along each eigenvector field in both directions to allow for the determination of σ_{max} . Practically we follow the approach described by Hlawitschka et al. [14] that we summarize here for completeness.

Bidirectional integration associates each initial location \mathbf{x}_0 with two end positions \mathbf{x}_1 and \mathbf{x}_2 . As previously pointed out, the lack of globally valid orientation of the eigenvector field implies that the respective order of these positions is arbitrary. Hence to compute the Jacobian of the flow map in each direction $\mathbf{J}_{\mathbf{x}}(t, t_0, \mathbf{x}_{1,2})$, we record at each point the vector chosen locally to play the role of forward direction. This vector is then used in a subsequent step to determine what indices should be used to compute the two Jacobian values through central differences.

The integration length (denoted t by analogy with the vector case) is a spatial scale parameter that must be selected carefully to reveal interesting structures. Excessive values not only lead increase the complexity of the characterized structures (by compounding the impact on multiple manifolds on individual trajectories), they also lead to issues associated with the boundaries of the domain. Indeed, trajectories whose requested length cannot be reached within the domain cause normalization issues in the computation of $\sigma_{1,2}$. Our solution to this problem consists in computing σ_{max} across a range of integration lengths in order to identify a posteriori the most relevant length. These discrete length samples can also be used to form a scale space in which a continuous analysis could be performed. Though we did not explore this avenue depth in the present work, we illustrate in the following section the incidence of this parameter on the resulting structures.

Once the FTLE fields have been computed, the next stage consists in extracting the ridges that form the salient manifolds of the tensor field's structure. We are using to that effect the method recently proposed by Barakat and Tricoche [1], in which the ridge extraction is formulated as a ray casting problem in a view-dependent setting. This method offers indeed the significant benefit of running interactively on the GPU, thus allowing us to test the implications of various parameters used to filter the ridges.

5 Results

To show the relationship between the separatrices of tensor field topology and the LCS computed in eigenvector fields we first consider the double point load dataset that has been studied in previous work [34, 35, 36, 37] since it provides a basis for comparison. Specifically, we applied the method described by Zheng et al. [36] to extract separating surfaces along the degenerate lines of the topology. These degenerate lines are shown as red curves in the images below. Unfortunately, this method turned out to be numerically challenging in the context of this particular dataset, as shown next.

We start by looking at the structures associated with the major eigenvector field, see Figure 5. It can be seen that the separatrices of the topology were only incompletely characterized, owing to the near degeneracy of the tensor field in the entire region surrounding the upper part of the P-type degenerate lines. As expected, the ridges of the FTLE field in contrast prove much more robust and properly capture the symmetric geometry of the separatrices. A close-up (Figure 5, bottom row)

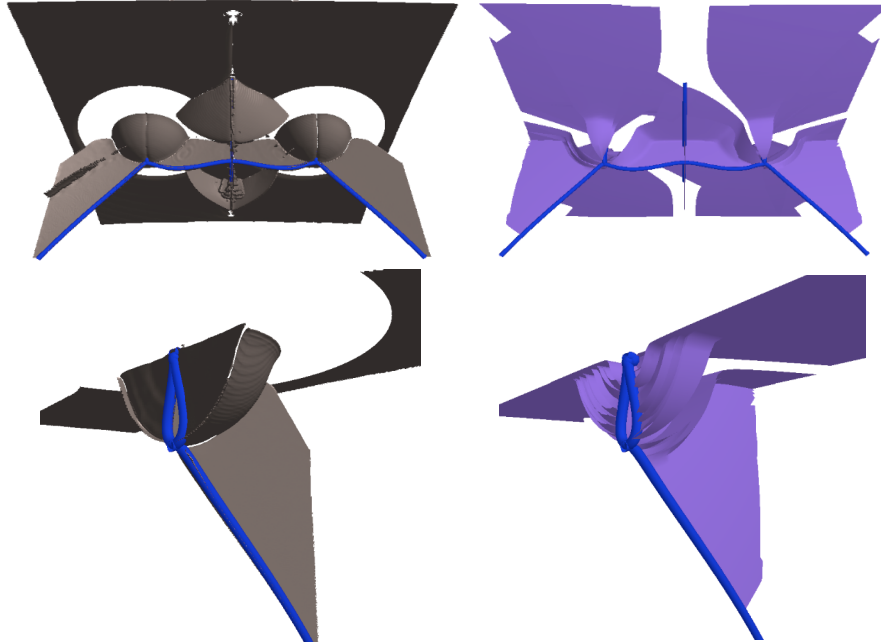


Fig. 5 Comparison between the separating surfaces associated with planar type (blue) degenerate lines and LCS computed in the major eigenvector field of the double point load dataset. Left: Ridges of FTLE. Right: separating surfaces and their corresponding degenerate lines.

sheds some additional light on the issues associated with the topology. It can indeed be observed that the separating surfaces are starting along inconsistent directions.

Again, the LCS do not suffer from this shortcoming. The topology associated with the minor eigenvector field (linear type degenerate lines) is shown in Figure 6.

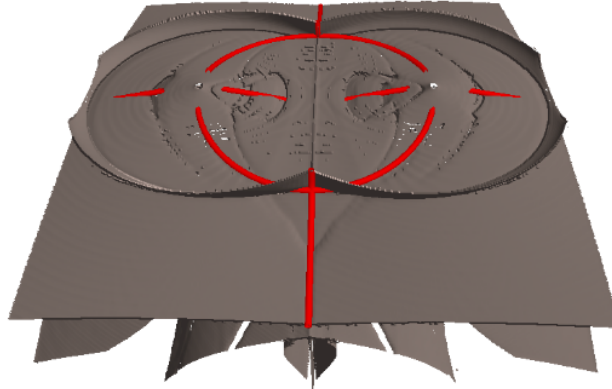


Fig. 6 Separatrices of the planar-type degenerate lines of the double point load dataset extracted as ridges of the minor eigenvector field

As mentioned previously, the integration length used in the construction of the FTLE field is a degree of freedom of the analysis that can be tuned to control the geometric complexity of the structures. We document the impact of this parameter on the resulting visualization in Figure 7 where the topology of the minor eigenvector field can be seen increase monotonically with the integration length.

While topology has been shown in previous work [27] to yield fragile and therefore unreliable structures in the context of noisy numerical datasets, our proposed approach is fundamentally more robust and enables the analysis of challenging engineering datasets. To document the performance of our method in such demanding scenarios, we considered two CFD simulations exhibiting turbulent flows in canonical configurations. The first dataset correspond to a single time step out of a transient simulation of a flow past a protruding cone, leading to the formation of downstream vortices. In the second dataset fast and slow fluid flow layers mix after passing a thin plate. The shear induced by the differing velocities causes strong turbulence. In these flow phenomena, the considered symmetric tensor field is the rate of strain, which is known to be closely related to major features of interest such as vortices and flow separation in fluid dynamics problems [10].

The surfaces characterized in those datasets form boundaries between regions of different strain behaviors, whereby each region is associated with a locally uniform pattern of a principal strain direction. The interpretation of the role of these regions and associated boundaries in the behavior of the flow in turn depends on additional parameters such as the relative magnitude of the eigenvalues, i.e. the tensor field anisotropy. Note that while these quantitative considerations are basically orthogo-

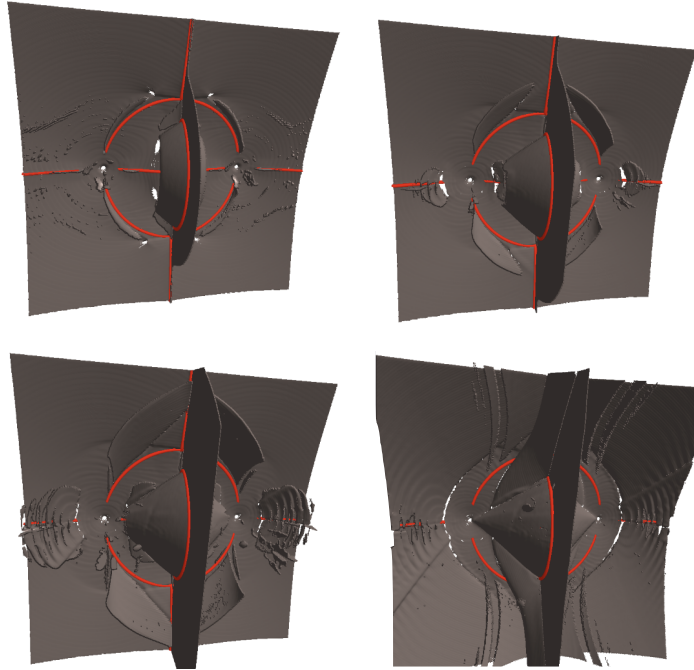


Fig. 7 Evolution of the extracted manifolds under increasing integration length in the minor eigenvector field of the double point load dataset.

nal to the structure of the eigenvector fields, they offer a complementary perspective that is key to a physical analysis of the considered phenomenon.

We start by considering the simpler of the two datasets, in which a protuberant cone causes vortex shedding. An illustration of the resulting vortices is presented in Figure 8.

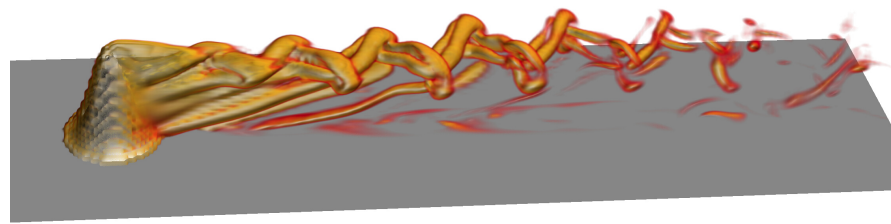


Fig. 8 Vortex shedding through a cone obstacle.

To reveal the relationship between the salient manifolds in the tensor FTLE field and the patterns of coherent orientation of the strain principal direction, we show in Figure 9 color coding of the eigenvector orientation (using the standard symmetric RGB encoding) combined with the geometry of those manifolds. It can be seen



Fig. 9 Major eigenvector of the strain tensor in shedder dataset combined with salient surfaces of tensor FTLE.

that these surfaces (shown in a 2D slice) properly delineate regions of different behaviors, corresponding to different colors. A 3D view of the surfaces is shown in Figure 10.

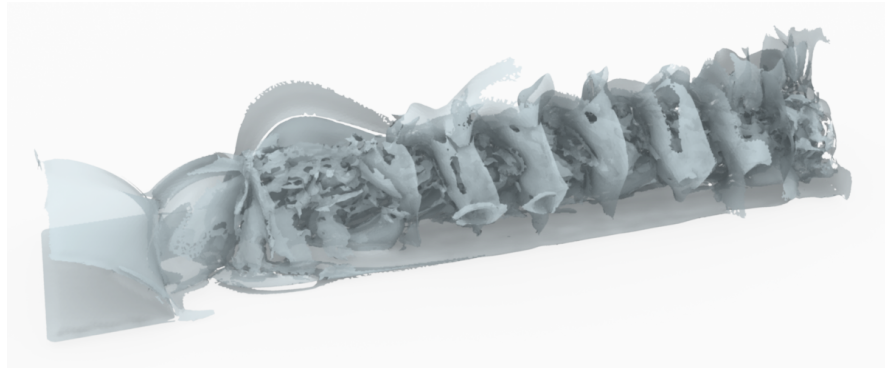


Fig. 10 Salient structures in major eigenvector field of shedder dataset.

The plate dataset considered hereafter exhibits significantly more complicated structures due to higher turbulence. This leads to convoluted patterns of the major eigenvector field of the strain tensor that are visible in Figure 11. Here again the salient surfaces obtained through Lagrangian processing successfully highlight the boundaries of significantly different regions and their impact on the flow.

A detailed 3D view of this dataset is proposed in Figure 12. The patterns of the flow itself (top left), as characterized through the standard LCS approach computed in the velocity vector field at fixed time, shows the typical turbulent patterns that are expected in this case. The major eigenvalue of the strain tensor (lower left) takes on high values that are directly correlated with the location of these structures. Hence

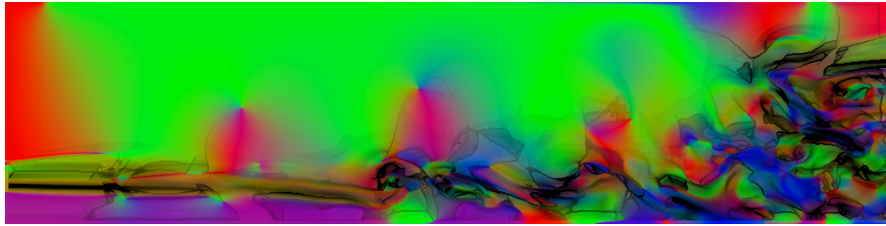


Fig. 11 Major eigenvector of the strain tensor in plate dataset and associated salient surfaces.

we use this field as a mask to spatially confine the Lagrangian computation of salient structures. The result is shown on the right hand side in Figure 12. It can be seen that very complicated geometric structures emerge from this analysis. Further investigation would be necessary to determine their role in the organization of the flow. As stated previously, such a study requires to take into account the influence of the eigenvalues and their interplay with the geometry of the eigenvector field.

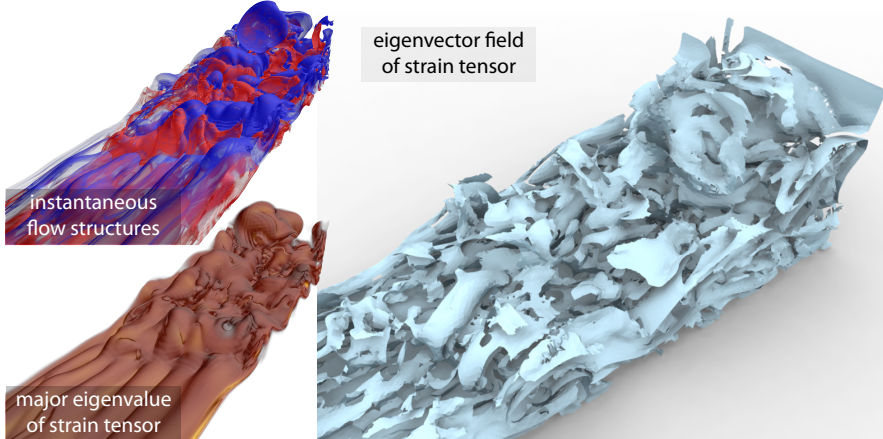


Fig. 12 **Plate dataset.** The top left image shows a overview of the instantaneous flow structures formed by the interaction of a shearing flow with a plate obstacle. The resulting turbulence induces the effective mixing of slow and fast moving layers. The bottom left image corresponds to the major eigenvalue of the strain tensor field. The right image shows the ridge surfaces extracted from the FTLE field computed in the strain tensor field.

6 Conclusion and Future Work

We have presented a generalization to tensor fields of Lagrangian coherent structures, a dynamical systems' concept applied so far to the analysis of vector fields.

Our proposed approach is built upon a Lagrangian metaphor for eigenvector fields that finds its theoretical justification in the connection that exists between vector fields and line fields. After reviewing the state of the art of structure-based tensor field visualization techniques, we have shown that LCS improve upon the results achieved by the topological method in a standard benchmark synthetic dataset. More importantly, our results document the ability of a LCS-based analysis to reveal salient structures in highly complex 3D tensor fields, such as those associated with large-scale CFD simulations of turbulent flows. This latter aspect opens promising avenues for future research as this new structure model appears to overcome the limitations that have so far strongly restricted the relevance of the topological method in demanding application scenarios.

Acknowledgements

This work was supported in part by a gift from Intel Visual Computing initiative.

References

1. S. Barakat and X. Tricoche. An image-based approach to interactive crease extraction and rendering. *Procedia Computer Science*, 1(1):1709 – 1718, 2010. ICCS 2010.
2. J. C. Criscione, J. D. Humphrey, A. S. Douglas, and W. C. Hunter. An invariant basis for natural strain which yields orthogonal stress response terms in isotropic hyperelasticity. *Journal of Mechanics and Physics of Solids*, 48:2445–2465, 2000.
3. M. de Saint-Venant. Surfaces à plus grande pente constituées sur des lignes courbes. *Bulletin de la Société Philomathématique de Paris*, pages 24–30, 1852.
4. T. Delmarcelle and L. Hesselink. The topology of symmetric, second-order tensor fields. In *Proceedings of IEEE Visualization 1994*, pages 140–147. IEEE Computer Society Press, 1994.
5. D. Eberly. *Ridges in Image and Data Analysis*. Kluwer Academic Publishers, 1996.
6. D. Eberly, R. Gardner, B. Morse, and S. Pizer. Ridges for image analysis. *Journal of Mathematical Imaging and Vision*, 4:351–371, 1994.
7. J. D. Furst and S. M. Pizer. Marching ridges. In *Proceedings of 2001 IASTED International Conference on Signal and Image Processing*, 2001.
8. J. D. Furst, S. M. Pizer, and D. H. Eberly. Marching cores: A method for extracting cores from 3d medical images. In *Proceedings of IEEE Workshop on Mathematical Methods in Biomedical Image Analysis*, pages 124–130, 1996.
9. A. Globus, C. Levit, and T. Lasinski. A tool for visualizing the topology if three-dimensional vector fields. In *IEEE Visualization Proceedings*, pages 33 – 40, October 1991.
10. R. Haimes. Using residence time for the extraction of recirculation regions. *AIAA Paper 99-3291*, 1999.
11. G. Haller. Lagrangian structures and the rate of strain in a partition of two-dimensional turbulence. *Physics of Fluids*, 13(11), 2001.
12. J. Helman and L. Hesselink. Surface representation of two and three-dimensional fluid flow topology. In *Proceedings of IEEE Visualization '90 Conference*, pages 6–13, 1990.
13. L. Hesselink, Y. Levy, and Y. Lavin. The topology of symmetric, second-order 3D tensor fields. *IEEE Transactions on Visualization and Computer Graphics*, 3(1):1–11, 1997.

14. M. Hlawitschka, C. Garth, X. Tricoche, G. Kindlmann, G. Scheuermann, K. Joy, and B. Hamann. Direct visualization of fiber information by coherence. *International Journal of Computer Assisted Radiology and Surgery*, 5(2):125ff, April 2010.
15. G. Kindlmann, R. San Jose Estepar, S. M. Smith, and C.-F. Westin. Sampling and visualizing creases with scale-space particles. *IEEE Transactions on Visualization and Computer Graphics*, 15(6):1415–1424, 2009.
16. G. Kindlmann, X. Tricoche, and C.-F. Westin. Delineating white matter structure in diffusion tensor MRI with anisotropy creases. *Medical Image Analysis*, 11(5):492–502, October 2007.
17. J. J. Koenderink and A. J. van Doorn. Local features of smooth shapes: ridges and courses. In B. C. Vemuri, editor, *Proc. SPIE Vol. 2031, p. 2-13, Geometric Methods in Computer Vision II, Baba C. Vemuri; Ed.*, pages 2–13, June 1993.
18. R. S. Laramee, H. Hauser, L. Zhao, , and F. H. Post. Topology-based flow visualization, the state of the art. In Mathematics and Visualization, editors, *Topology-Based Methods in Visualization II*, pages 1–19. Springer-Verlag, 2007.
19. W. E. Lorensen and H. E. Cline. Marching cubes: A high resolution 3d surface construction algorithm. *Computer Graphics*, 21(4):163–169, 1987.
20. J. E. Marsden and A. J. Tromba. *Vector Calculus*. W.H. Freeman and Company, New York, New York, 1996.
21. B. S. Morse. *Computation of Object Cores from Grey-Level Images*. PhD thesis, University of North Carolina at Chapel Hill, Chapel Hill, NC, 1994.
22. R. Peikert and M. Roth. The Parallel Vectors operator - a vector field visualization primitive. In *IEEE Visualization Proceedings '00*, pages 263 – 270, 2000.
23. M. Roth. *Automatic Extraction of Vortex Core Lines and Other Line-Type Features for Scientific Visualization*. PhD thesis, ETH Zürich, 2000.
24. F. Sadlo and R. Peikert. Efficient visualization of lagrangian coherent structures by filtered amr ridge extraction. *IEEE Trans. Vis. Comput. Graph.*, 13(6):1456–1463, 2007.
25. J. Sahner, T. Weinkauf, and H.-C. Hege. Galilean invariant extraction and iconic representation of vortex core lines. In K. J. K. Brodlie, D. Duke, editor, *Proc. Eurographics / IEEE VGTC Symposium on Visualization (EuroVis '05)*, pages 151–160, Leeds, UK, June 2005.
26. G. Scheuermann and X. Tricoche. Topological methods in flow visualization. In C. Johnson and C. Hansen, editors, *Visualization Handbook*, pages 341–356. Academic Press, 2004.
27. T. Schultz, H. Theisel, and H.-P. Seidel. Topological visualization of brain diffusion MRI data. *IEEE Transactions on Visualization and Computer Graphics*, 13(6):1496–1503, 2007.
28. T. Schultz, H. Theisel, and H.-P. Seidel. Create surfaces: From theory to extraction and application to diffusion tensor MRI. *IEEE Transactions on Visualization and Computer Graphics*, 2009. RapidPost, accepted 16 April 2009. doi 10.1109/TVCG.2009.44.
29. M. Spivak. *A Comprehensive Introduction to Differential Geometry, Volume III*. Publish or Perish Inc., 1979.
30. G. D. Stetten. Medial-node models to identify and measure objects in real-time 3-d echocardiography. *IEEE Transactions on Medical Imaging*, 18(10):1025–1034, 1999.
31. H. Theisel and H.-P. Seidel. Feature flow fields. In *Proceedings of Joint Eurographics - IEEE TCVG Symposium on Visualization (VisSym '03)*, pages 141–148, 2003.
32. X. Tricoche, G. Kindlmann, and C.-F. Westin. Invariant crease lines for topological and structural analysis of tensor fields. *IEEE Transactions on Visualization and Computer Graphics*, 14(6):1627–1634, 2008.
33. X. Tricoche, X. Zheng, and A. Pang. Visualizing the topology of symmetric, second-order, time-varying two-dimensional tensor fields. In J. Weickert and H. Hagen, editors, *Visualization and Processing of Tensor Fields*, pages 225–240. Springer, 2006.
34. X. Zheng and A. Pang. Topological lines in 3D tensor fields. In *VIS '04: Proceedings of the conference on Visualization '04*, pages 313–320, Washington, DC, USA, 2004. IEEE Computer Society.
35. X. Zheng, B. Parlett, and A. Pang. Topological lines in 3D tensor fields and discriminant hessian factorization. *IEEE Transactions on Visualization and Computer Graphics*, 11(4):395–407, 2005.

36. X. Zheng, B. Parlett, and A. Pang. Topological structures of 3d tensor fields. In *Proceedings of IEEE Visualization*, pages 551–558, 2005.
37. X. Zheng, X. Tricoche, and A. Pang. Degenerate 3d tensors. In *Visualization and Processing of Tensor Fields*, pages 241–256. Springer, 2006.